An experimental setup for wave-body forces in shear currents

Benjamin K. Smeltzer, Eirik Æsøy, Yan Li, Simen Å. Ellingsen

Department of Energy and Process Engineering
Norwegian University of Science and Technology
Kolbjorn Hejes vei 2, N-7491 Trondheim, Norway
benjamin.smeltzer@ntnu.no

1 Introduction

Understanding and characterizing wave-body forces in the complex marine environment is an ongoing challenge. We herein consider the effects of a sub-surface shear current, which alters wave dispersion and thus influences the interactions between waves and bodies. Considering ships as an example case study, previous theoretical and numerical work has shown that qualitative features of wakes such as the wake angle as well as the wave resistance are impacted by the presence of a sub-surface shear current[1, 2]. Wave resistance values have been shown to be significantly altered for realistic model vessels traveling atop measured strongly sheared currents at the mouth of the Columbia River compared to a depth-uniform current with the same surface velocity[3]. The results highlight the need to better understand the three-way interaction between waves, bodies, and shear currents. We have developed a laboratory setup for generating shear currents that enables study of wave-body interactions in depth-varying flows. Preliminary results and plans for further work are presented here. Although the work focuses on studying ship wakes and wave resistance, the experimental methods can readily be extended to studying other model structures in future efforts.

2 Experimental Methods

Shear currents were generated in a laboratory wave tank using a pump system to induce flow over a transparent plate of dimension 2×2 m, shown in Fig. 1. A combination of honeycomb flow straighteners and a curved wire mesh was used to produce a shear flow at downstream locations. The vertical profile of the flow-wise current was measured using a light-emitting diode (LED)-based particle image velocimetry (PIV) system similar to that described in Willert et al.[4], consisting of a high power LED (Luminus PT-120-TE), fiber array, and collimation lens to produce a pulsed light sheet. The water was seeded with 40 μm polystyrene spheres, and fluid velocities in the streamwise direction were obtained by processing images from a camera (Imperx Bobcat 1610) mounted out of the plane as shown in Fig. 1. The position of the light sheet can be translated to measure the current profile at various flow and spanwise locations.

Waves were produced using a pneumatic wave maker discharging bursts of air at a computer-controlled frequency and 50% duty cycle. The resulting free surface gradient field was measured using a synthetic Schlieren (SS) method[5], with a random dot pattern mounted below the transparent plate and imaged from a camera located above ($\sim$ 2 m optical path length) the water surface. Images of the dots were processed using a windowed digital image correlation technique, where the resulting shifts of the dots determine the local free surface gradient.

The effects of the shear current on wave dispersion were measured by stepping the pneumatic wave maker through frequencies 2-6 Hz as a function of time and recording the surface gradient using the

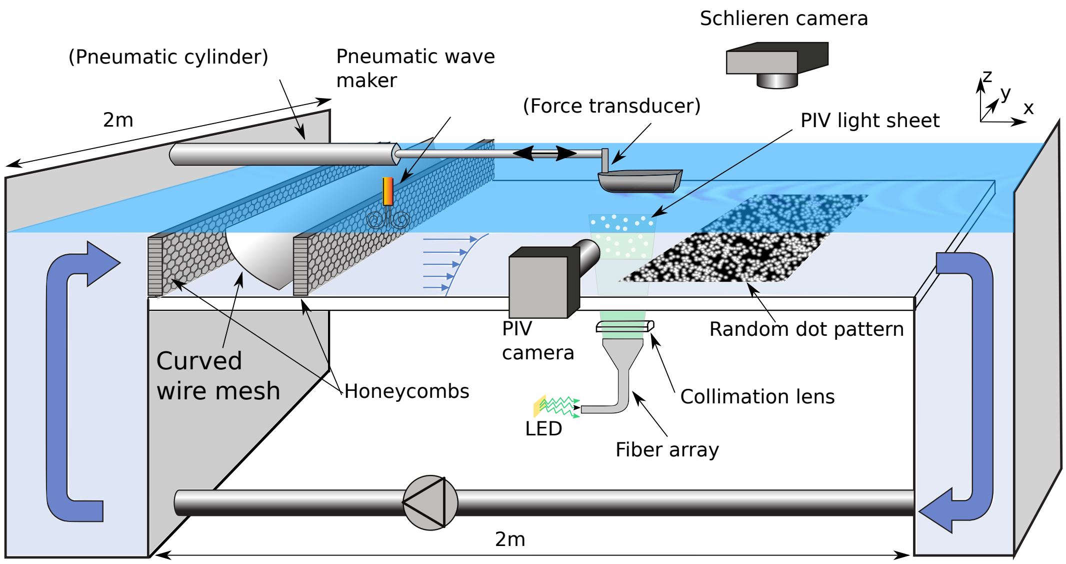

Figure 1: Experimental setup. Yet-to-be implemented components are shown in parentheses.

SS-method, which was then processed to find the linear dispersion relation. For the early results reported herein, the wave maker was positioned just downstream of the honeycomb structure (upstream of the random dot pattern), producing waves with wave vectors primarily in the downstream direction, hereafter defined as the x-axis. Ten second windows (corresponding to the length of time the driving frequency was kept constant) were analyzed yielding gradients $\nabla\eta^j(x,y,t) \equiv [\eta_x^j(x,y,t), \eta_y^j(x,y,t)]$ where the superscript denotes the j-th frequency window. As the primary wave components were traveling along the x-axis, η_y^j was disregarded for simplicity. Performing a fast Fourier transform (FFT) in space and time of $\eta_x^j(x,y,t)$ gives the frequency-wavenumber spectrum $\tilde{\eta}_x^j(k_x,k_y,\omega)$. Assuming small-amplitude waves, maximum values of $|\tilde{\eta}_x^j(k_x,k_y,\omega)|^2$ are concentrated along the linear dispersion relation surface $\omega(k_x,k_y)$. Discrete points on the dispersion surface for downstream waves ($k = k_x$) were obtained by performing a Gaussian fit to extract peaks of $|\tilde{\eta}_x^j(k,0,\omega)|^2$ for frequencies $\omega = \omega^j$ and higher harmonics. Analyzing the entire time series of $\eta_x^j(x,y,t)$ thus yields a set of wavenumbers k^i and associated phase velocities $c^i_{\mathrm{EXP}} = \omega^i/k^i$.

Also depicted in Fig. 1 are yet-to-be implemented plans for measurements of ship waves and wave resistance. A pneumatic cylinder will be used to tow a small model ship mounted to a force transducer. The wake pattern can be measured at selected locations using the SS-technique described above. The system is expected to enable measurement of wake surface profile and wave resistance forces at relevant Froude numbers (approximately 0.15-0.5), with comparison to depth-uniform current results. For sufficiently shallow draught the drag not due to waves should be nearly independent of the shear, allowing isolation of the the wave resistance contribution. The orientation of the towing system can be moved to study different angles of ship motion in both upstream and downstream directions.

3 Theoretical Methods

We work in a coordinate system with horizontal directions $\mathbf{r} = [x,y]$ and vertical dimension z as shown in Fig. 1, and assume a background flow $\mathbf{U}(z)$ varying only with depth z (not with x and y). The dispersion relation for linear waves propagating atop such a flow can be expressed[3]:

$$(1+I_g)\,(\omega-\mathbf{k}\cdot\mathbf{U}_0)^2 + (\omega-\mathbf{k}\cdot\mathbf{U}_0)\,\mathbf{k}\cdot\mathbf{U}_0'\tanh kh/k - \omega_0^2 = 0 \tag{1}$$

$$I_g(\mathbf{k}) = \int_{-h}^{0} dz \frac{\mathbf{k}\cdot\mathbf{U}''w(\mathbf{k},z,0)\sinh k(z+h)}{k[\mathbf{k}\cdot\mathbf{U}(z)-\omega]w(\mathbf{k},0,0)\cosh kh}, \tag{2}$$

where $\mathbf{k} = [k_x, k_y]$ is the wavevector, $k = |\mathbf{k}|$, ω the wave frequency, and h the constant mean water depth. $w(\mathbf{k}, z, t)$ is the vertical velocity of the wave (see Ref. [3]) and $\omega_0^2 = \left(gk + \sigma k^3/\rho\right) \tanh kh$ is the dispersion relation in quiescent waters with surface tension coefficient σ and density ρ. The system of equations (1) and (2) is solved for unknowns ω and w using an iterative direct-integration method (DIM)[6, 7].

We wish to consider ship waves in the presence of the background shear profile. The 'ship' is approximated as a moving externally applied pressure distribution at the free surface[2, 8], $\hat{p}_{\text{ext}}(\mathbf{r}) = p_0 \exp(-\pi^2[(2x/L)^2 + (2y/B)^2]^3)$, where $\mathbf{r}$ is expressed in a reference frame moving with the ship, and L and B represent the length and beam of the ship respectively. The resulting ship wake surface elevation is [3]:

$$\zeta(\mathbf{r}) = \frac{1}{\rho} \int \frac{d^2k}{(2\pi)^2} \frac{k p_{\text{ext}}(\mathbf{k}) F(\mathbf{k})}{(\omega_+ - i\epsilon)(\omega_- - i\epsilon)} \mathrm{e}^{i\mathbf{k}\cdot\mathbf{r}}, \tag{3}$$

where $F(\mathbf{k}) = \tanh kh/(1 + I_g)$, and $p_{\text{ext}}(\mathbf{k})$ is the pressure distribution in Fourier space. $\omega_\pm$ are the frequencies of waves traveling parallel and anti-parallel to $\mathbf{k}$, found numerically from (1) and (2), while $\epsilon = 0^+$ is a small parameter necessarily to satisfy the radiation condition[2].

The wave resistance can be found as [2, 8]:

$$R = -\frac{1}{V} \int d^2r p_{\text{ext}}(\mathbf{r}) \mathbf{V} \cdot \nabla\zeta(\mathbf{r}) = -\frac{i}{\rho V} \int \frac{d^2k}{(2\pi)^2} \frac{k(\mathbf{k}\cdot\mathbf{V})|p_{\text{ext}}(\mathbf{k})|^2 F(\mathbf{k})}{(\omega_+ - i\epsilon)(\omega_- - i\epsilon)}, \tag{4}$$

where $\mathbf{V}$ is the ship velocity, and $V = |\mathbf{V}|$.

4 Results

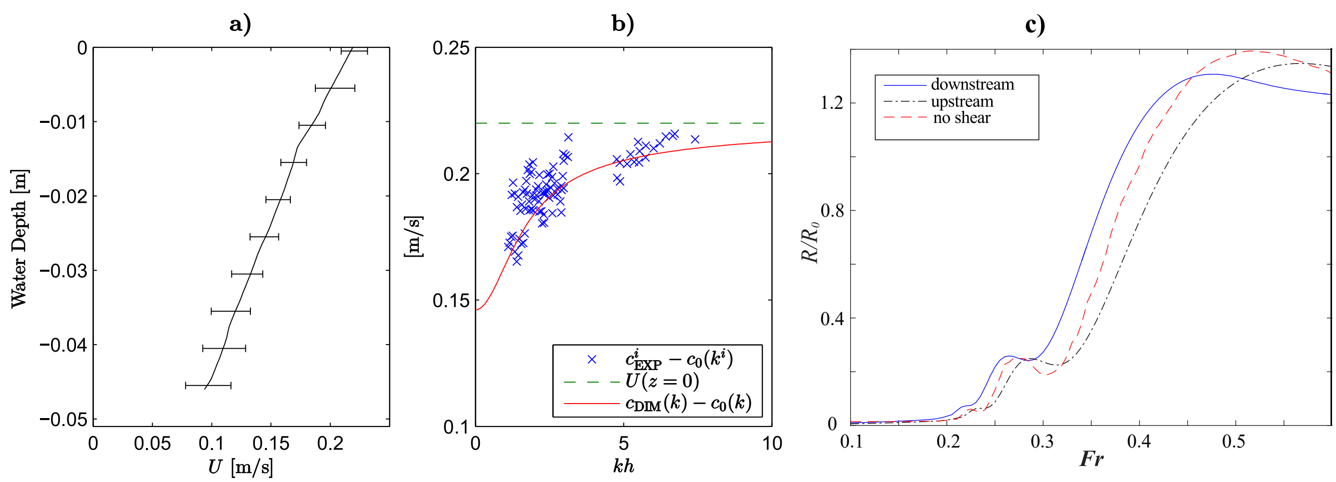

Figure 2: a) Current profile as a function of depth as measured by PIV. b) Measured phase velocities (x-marks) as a function of kh, compared to c_0, the value for a uniform current $U(z) = U_0$. The dashed curve shows the measured surface current U_0, while the solid curve is the dispersion relation calculated by the DIM assuming the current profile from a). c) Calculated wave resistance normalized to R_0 as a function of $Fr = V/\sqrt{gL}$ of a model ship with length $L = 15$ cm and beam $B = 3$ cm traveling upstream (dashed-dotted line) and downstream (solid curve) atop the measured current profile in a). The case in uniform current (no shear) is shown as the dashed line. See text for details.

The mean streamwise velocity as a function of depth measured with PIV is shown in Fig. 2a. The "error bars" represent the range of values obtained at different locations within the wave measurement area extent. The measured phase velocities c^i_{EXP} of downstream propagating waves relative to quiescent waters $c_0(k) = \sqrt{(g/k + \sigma k/\rho) \tanh kh}$ are shown in Fig. 2b along with the dispersion relation calculated using the DIM assuming a current profile shown with a line in Fig. 2a. The dashed line is the surface current. The relative phase velocities for downstream waves on shear decay with decreasing kh in a manner roughly consistent with the predicted values calculated using the DIM.

In the interest of future measurements of ship wakes and wave resistance in the presence of shear currents it is useful to show an example calculation of the effects of the shear current generated here on the behavior of a ship wake. Fig. 2c shows the steady state wave resistance calculated using (3) and (4) for a model "ship" atop the measured laboratory shear current. The modeled ship has length $L = 15$ cm and beam $B = 3$ cm, using a supergaussian externally applied pressure distribution with the method of [3] and the DIM. The wave resistance is normalized to $R_0 = p_0^2/2\pi^3\rho g$ and is shown as a function of Froude number $Fr = V/\sqrt{gL}$ for upstream and downstream directions. The velocity V is defined relative to the surface velocity $U_0 = 0.22$ m/s. The dashed red curve also shows the wave resistance in the absence of shear (uniform current). The wave resistance is greatly affected by the presence of a subsurface shear current for $0.25 \lesssim Fr \lesssim 0.45$, consistent with the results from previous studies[2, 3]. These early results demonstrate the promise of future experimental measurements of the effects of shear on wave-body interaction.

5 Conclusion

We have presented the development of a laboratory setup for studying wave-body interactions in the presence of a sub-surface shear current. Methods implemented are able to produce and measure shear currents and waves. Theoretical prediction of wave resistance for a typical model ship on our measured example shear flow show large effects of shear of $0.25 \lesssim Fr \lesssim 0.45$. The magnitude of near-surface shear is sufficient to cause alterations to the wave resistance that can amount to a difference of a factor of two between upstream versus downstream ship motion for practical model ship sizes. Future work will involve implementation of a model ship towing system to study ship wakes and wave resistance atop the lab-generated shear flow.

References

[1] S. Å. Ellingsen, Ship waves in the presence of uniform vorticity, J. Fluid Mech. 742 (2014) R2.

[2] Y. Li and S. Å. Ellingsen, Ship waves on uniform shear current at finite depth: wave resistance and critical velocity, J. Fluid Mech. 791 (2016), 539–567.

[3] Y. Li, B. K. Smeltzer and S. Å. Ellingsen, Transient wave resistance upon a real shear current, European Journal of Mechanics / B Fluids (2017), http://dx.doi.org/10.1016/j.euromechflu.2017.08.012.

[4] C. Willert, B. Stasicki, J. Klinner and S. Moessner, Pulsed operation of high-power light emitting diodes for imaging flow velocimetry, Meas. Sci. Technol. 21 (2010), 075402.

[5] F. Moisy, M. Rabaid, and K. Salsac, A synthetic Schlieren method for the measurement of the topography of a liquid surface, Exp. Fluids 36 (2009) 1021-1036.

[6] Y. Li and S. Å. Ellingsen, Direct integration method for surface waves on a depth dependent flow, (manuscript in preperation).

[7] Y. Li, Surface water waves on depth dependent flows, PhD Thesis, NTNU (2017).

[8] T. H. Havelock, Wave resistance: some cases of three-dimensional fluid motion, Proc. R. Soc. London A, 95 (1919), 354–365.